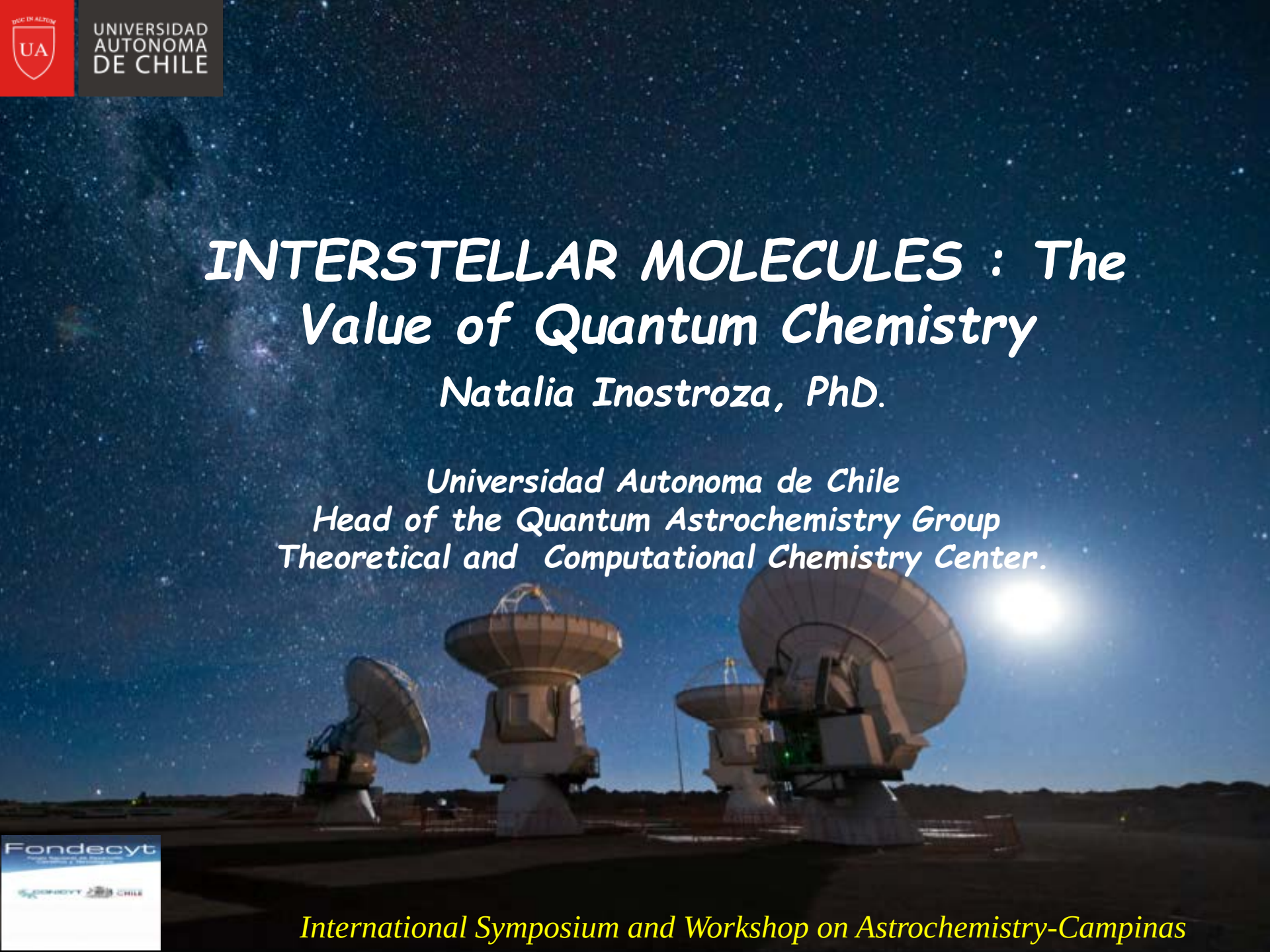

INTERSTELLAR MOLECULES : The Value of Quantum Chemistry

Natalia Inostroza, PhD.

Universidad Autonoma de Chile
Head of the Quantum Astrochemistry Group
Theoretical and Computational Chemistry Center.

International Symposium and Workshop on Astrochemistry-Campinas

2 atoms		3 atoms		4 atoms	5 atoms	6 atoms	7 atoms	8 atoms
H_2	NaCl	C_3	N_2H^+	c-C_3H	C_5	C_5H	C_6H	CH_3C_3N
AlF	OH	C_2H	N_2O	l-C_3H	C_4H	l-H_2C_4	CH_2CHCN	$HCOOCH_3$
AlCl	PN	C_2O	NaCN	C_3N	C_4Si	C_2H_4	CH_3C_2H	CH_3COOH
C_2	SO	C_2S	SO_2	C_3O	l-C_3H_2	CH_3CN	HC_5N	C_7H
CH	SO^+	CH_2	c-SiC_2	C_3S	c-C_3H_2	CH_3NC	CH_3CHO	H_2C_6
CH^+	SiO	HCN	CO_2	C_2H_2	CH_2CN	CH_3OH	CH_3NH_2	CH_2OHCHO
CN	SiS	HCO	NH_2	HCCN	CH_4	CH_3SH	c-C_2H_4O	l-HC_6H
CO	CS	HCO^+	CO_2^+	$HCNH^+$	HC_3N	HC_3NH^+	H_2CCHOH	CH_2CHCHO
CO^+	HF	HCS^+	H_3^+	HNCO	HC_2NH	HC_2CHO	C_6H^-	CH_2CCHCN
CP	SH	HOC^+	H_2D^+, HD_2^+	HNCS	HCOOH	NH_2CHO		NH_2CH_2CN
SiC	HD	H_2O	SiCN	$HOCO^+$	H_2CNH	C_5N		
HCl	FeO?	H_2S	AlNC	H_2CO	H_2C_2O	l-HC_4H		
KCl	O_2?	HNC	OCS	H_2CN	H_2NCN	l-HC_4N		
NH	CF^+	HNO	HCP	H_2CS	HNC_3	c-H_2C_3O		
NO	SiH?	MgCN	CCP	H_3O^+	SiH_4	H_2CCNH		
NS	PO	MgNC		NH_3	H_2COH^+			
				c-SiC_3	C_4H^-			
				CH_3	CNCHO			

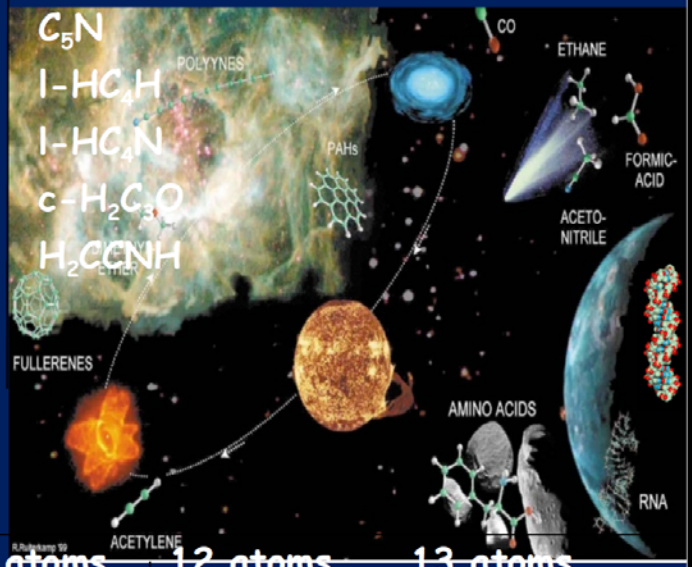

C_3N^-
PH_3

9 atoms			10 atoms	11 atoms	12 atoms	13 atoms
CH_3C_4H	CH_3CH_2OH	SiNC	CH_3C_5N	HC_9N	C_6H_6	$HC_{11}N$
CH_3CH_2CN	HC_7N	$CH_3C(O)NH_2$	$(CH_3)_2CO$	CH_3C_6H	$C_2H_5OCH_3$	
$(CH_3)_2O$	C_8H^-	CH_2CHCH_3				

What's it Good For?

- Computational chemistry is a rapidly growing field in chemistry.
  - Computers are getting faster.
  - Algorithms and programs are maturing.
- Some of the almost limitless properties that can be calculated with computational chemistry are:
  - Equilibrium and transition-state structures
  - dipole and quadrapole moments and polarizabilities
  - Vibrational frequencies, IR and Raman Spectra
  - NMR spectra
  - Electronic excitations and UV spectra
  - Reaction rates and cross sections
  - thermochemical data

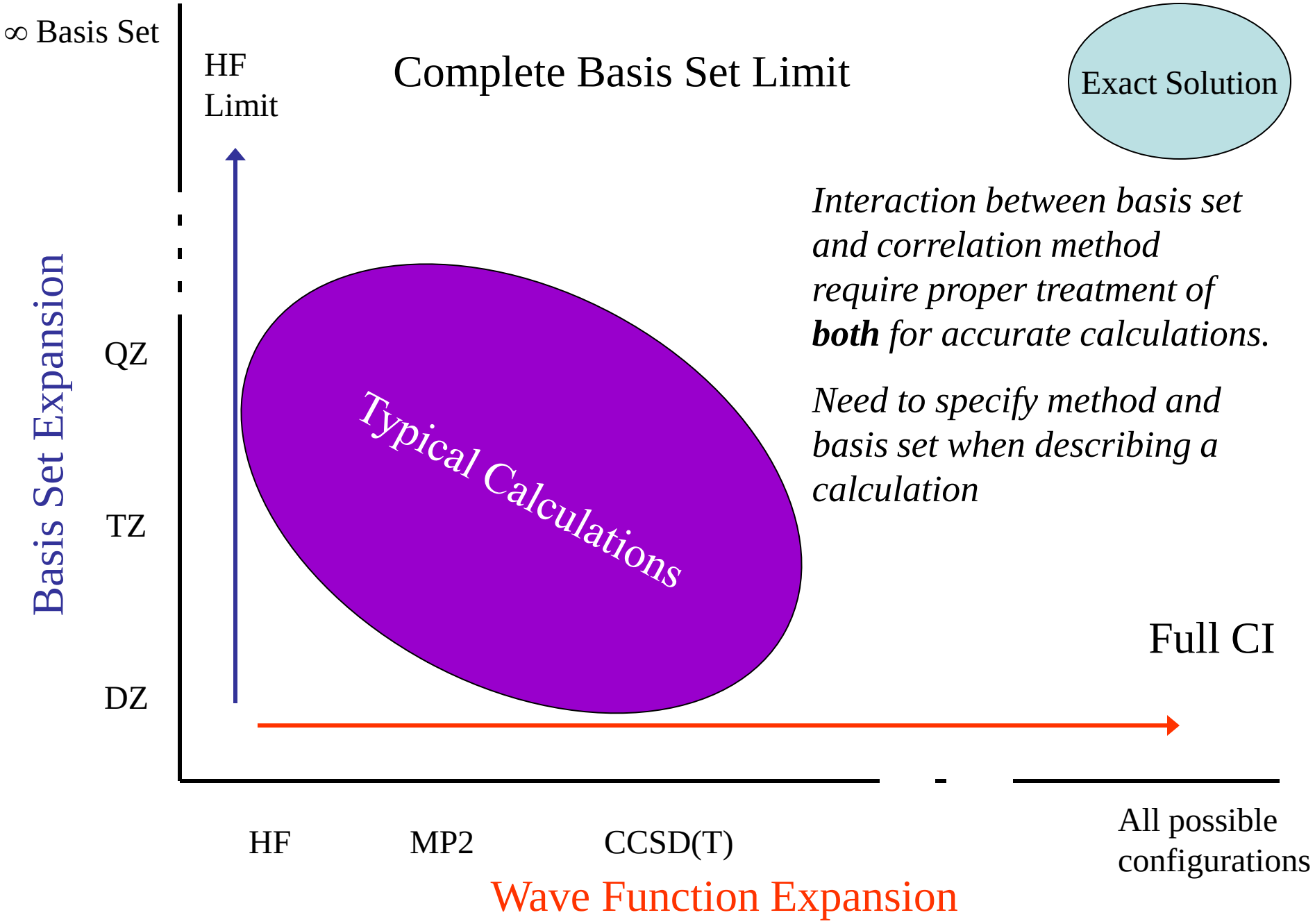
∞ Basis Set
HF Limit
Complete Basis Set Limit
Exact Solution
Interaction between basis set and correlation method require proper treatment of both for accurate calculations.
Need to specify method and basis set when describing a calculation
Basis Set Expansion
QZ
TZ
DZ
Typical Calculations
Full CI
HF
MP2
CCSD(T)
All possible configurations
Wave Function Expansion

Computational Cost

Why not use best available correlation method with the largest available basis set?

Method	Scaling of Cost
HF	$M^2 - M^3$
MP2	M^5
CCSD	M^6
CCSD(T)	M^7

- A MP2 calculation would be 100x more expensive than HF calculation with same basis set.
- A CCSD(T) calculation would be 10^4x more expensive than HF calculation with same basis set.
- Tripling basis set size would increase MP2 calculation 243x (3^5).
- Increasing the molecule size 2x (say ethane→butane) would increase a CCSD(T) calculation 128x (2^7).

Overview

- Different choices of methods and basis sets can yield a large variation in results.
- It is important to know the errors associated with and limitations of different computational approaches.
- This is important when doing your own calculations, and when evaluating the calculations of others.

- Don't just accept the numbers the computer spits out at face value!

Main Results

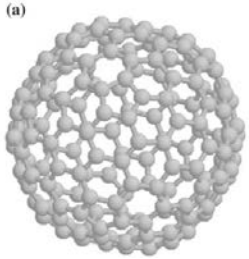

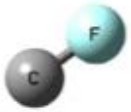

CF^+

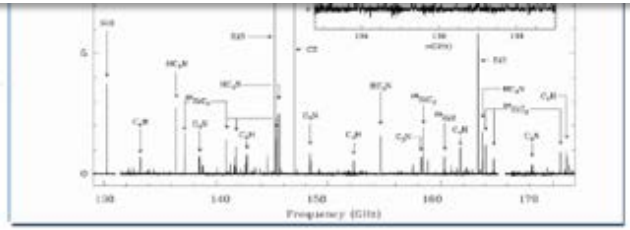

^{28}SiO ^{29}SiO ^{30}SiO

$^{28}SiF^+$ $^{29}SiF^+$ $^{30}SiF^+$

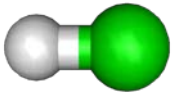

$H^{35}Cl$ $D^{35}Cl$ $T^{35}Cl$ $H^{37}Cl$ $D^{37}Cl$ $T^{37}Cl$

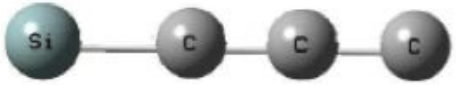

l-SiCCC l-CSiCC

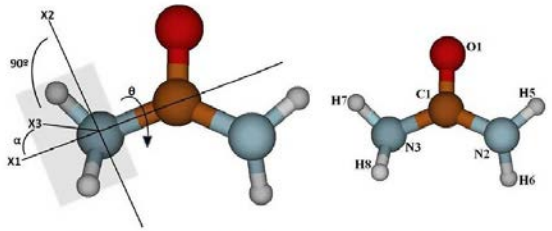

Figure 1. Structural parameters of Urea, definition of NH_2-torsion (θ) and NH_2-wagging (α) coordinates.

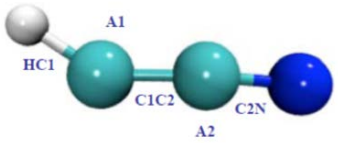

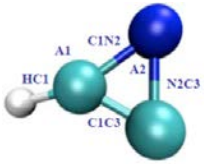

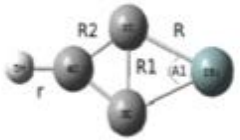

Results

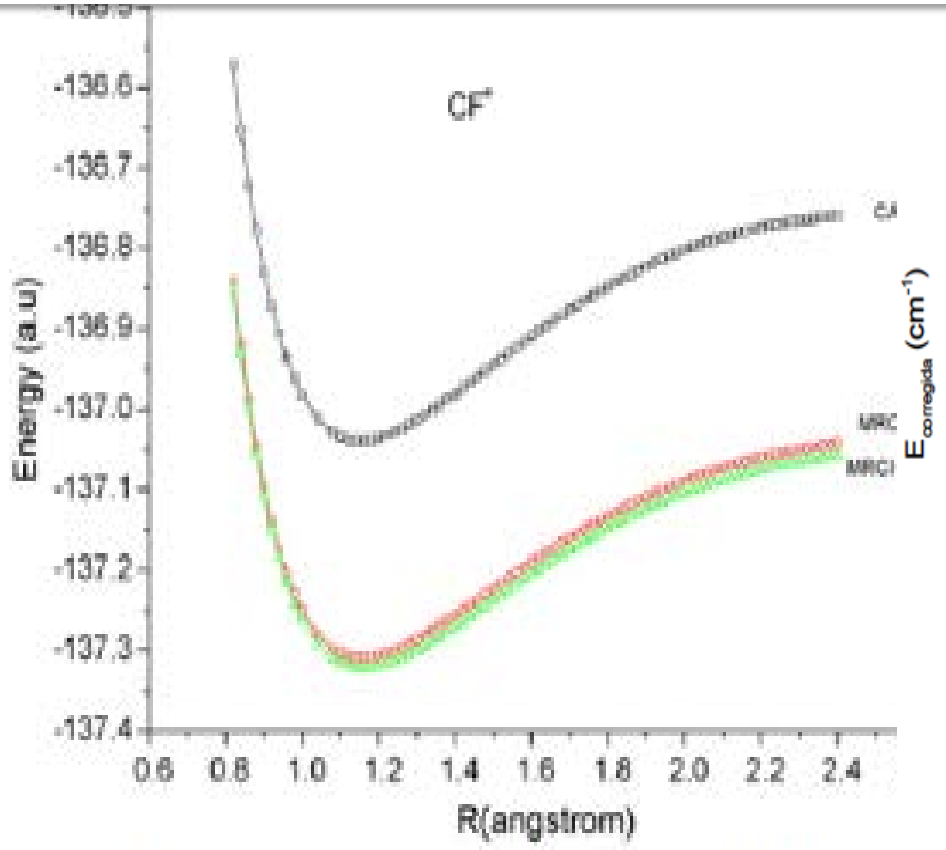

Fig. 1. Potential energy functions of CF^+, using aug-cc-pV5Z basis set.

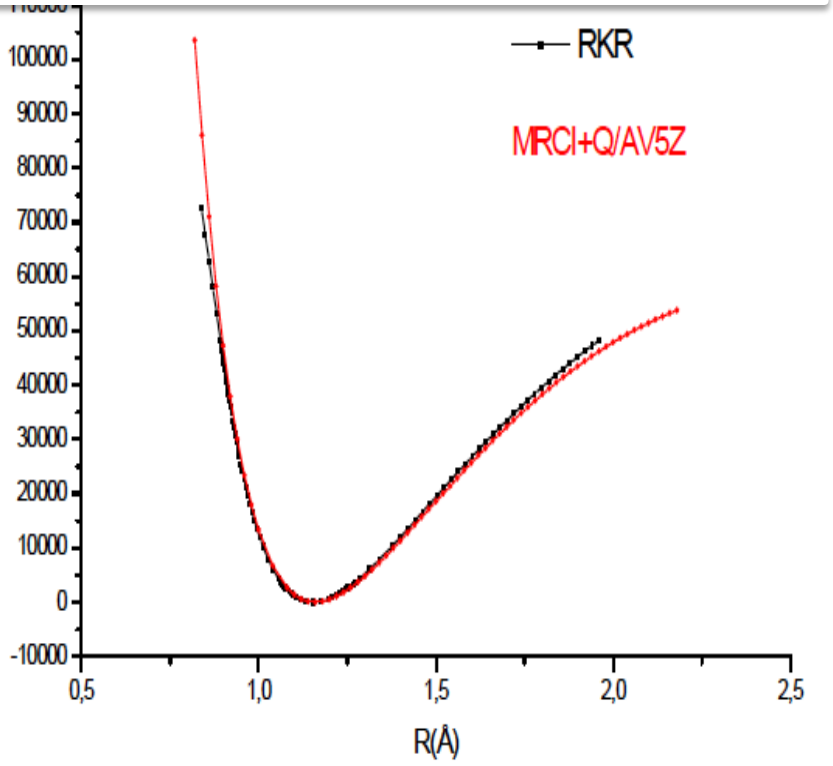

ΔECASSCF-MRCI =7.33 eV (169.203 kcal/mol),
ΔEMRCI-MRCI+Q=0.379 eV
(8.748 kcal/mol

MRCI+Q/aug-cc-pV5Z para el ión CF+ versus la curva calculada con el método Rydberg-Klein-Rees (RKR)

Results

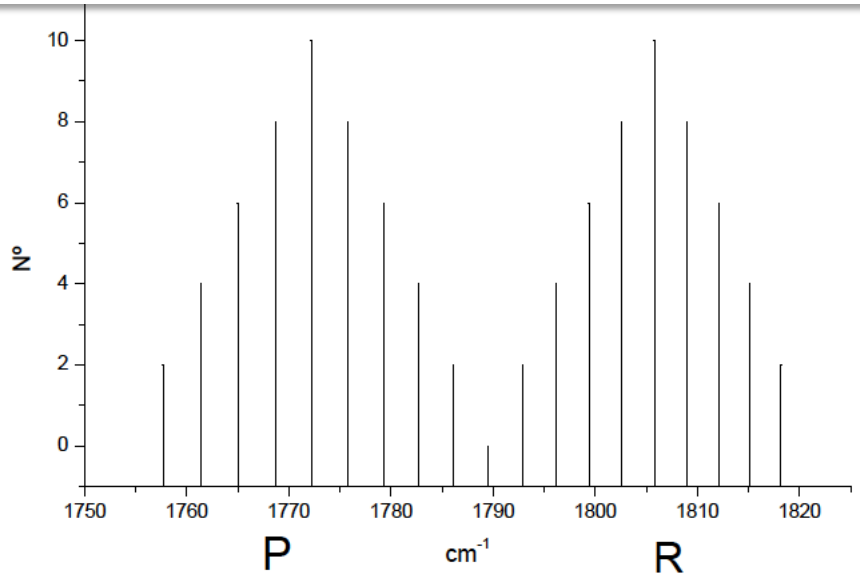

Be = 1.71662 cm^{-1} (MP).
Dunham Coeff.
Y01 =1. 71013 cm^{-1}

Be (Gruebele)
Y01 = 1.72041 cm-1.

J1/J	0	1	2	3	4	5	6	7	8	9
0	1789.5	1792.9(R0								
1	1786.1(P1		1796.2(R1							
2		1782.7(P2		1799.4(R2						
3			1779.3(P3		1802.6(R3					
4				1775.8(P4		1805.8(R4				
5					1772.2(P5		1809.0(R5			
6						1768.7(P6		1812.1(R6		
7							1765.0(P7		1815.1(R7	
8								1761.4(P8		1818.2(R8
9									1757.7(P9	

ν	$B_ν$
0	1.69066
1	1.67017
2	1.65137
3	1.63629
4	1.61299
5	1.53989

Results

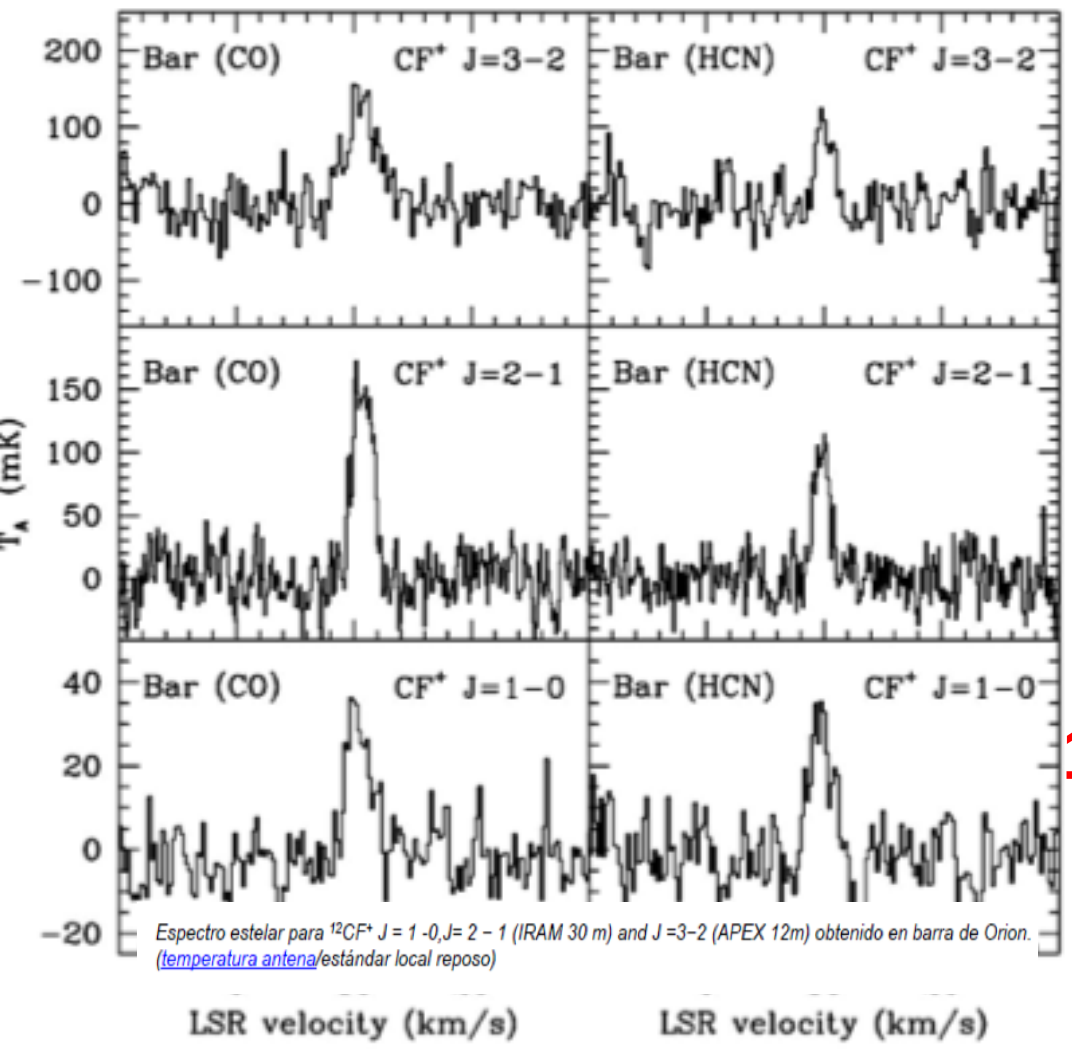

Espectro estelar para $^{12}CF^+$ J = 1 -0,J= 2 – 1 (IRAM 30 m) and J =3–2 (APEX 12m) obtenido en barra de Orion. (temperatura antena/estándar local reposo)

Rotational transitions

Our results	Obs.
304.2 [GHz]	307.7 [GHz]
203.1 [GHz]	205.2 [GHz]
102.0 [GHz]	102.6 [GHz]

$$\nu = 0, J_2 - J_1 = 1$$

N.Inostroza, J.R.Letelier, P.Fuentealba, M.L.Senent,
***Spectrochimica* Acta Part A-Molec. and Biomolecular Spectroscopy, 71, 798 (2008).**

Silicon Carbon Molecules

Molecular Astrophysics:
Silicon carbon molecules have been identified in gas phase. (Si is a major constituent of interstellar dust)

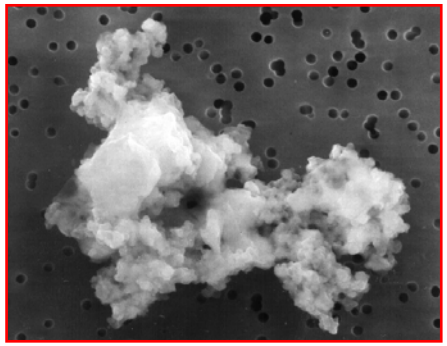

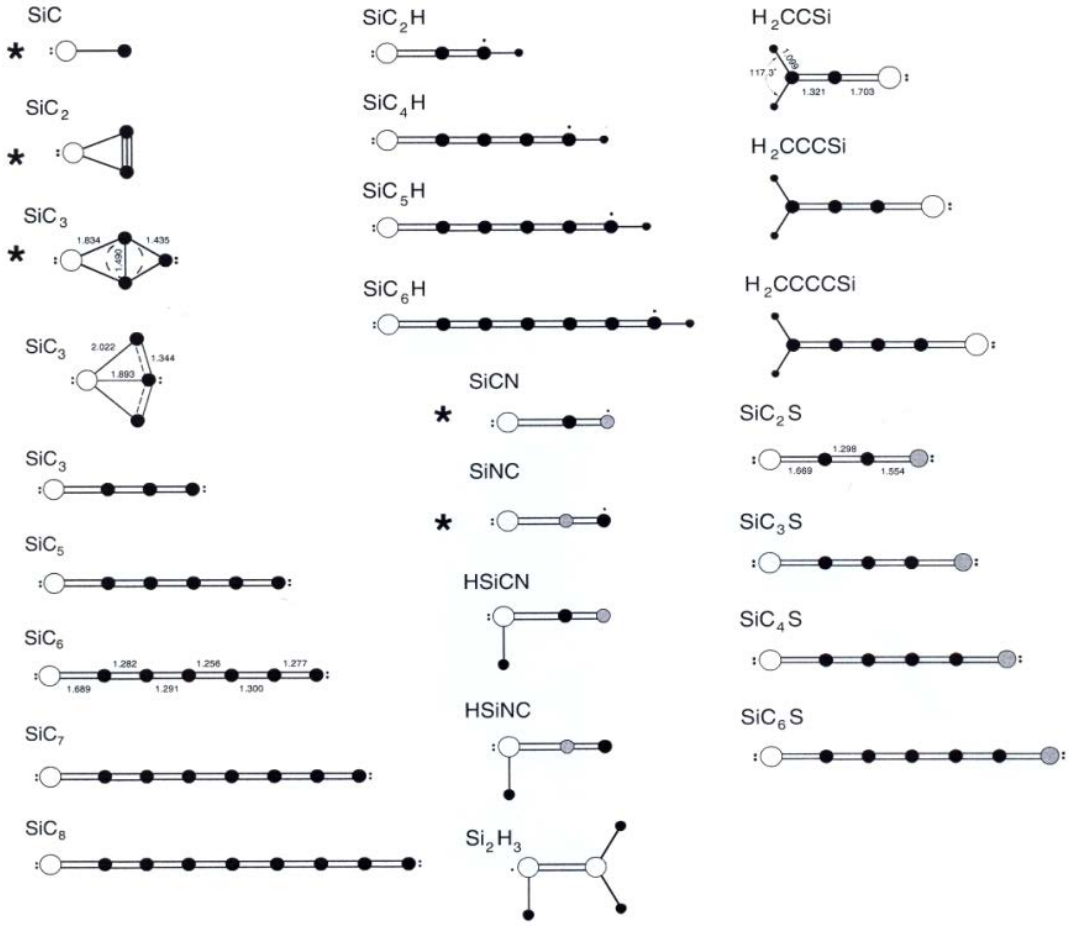

Results

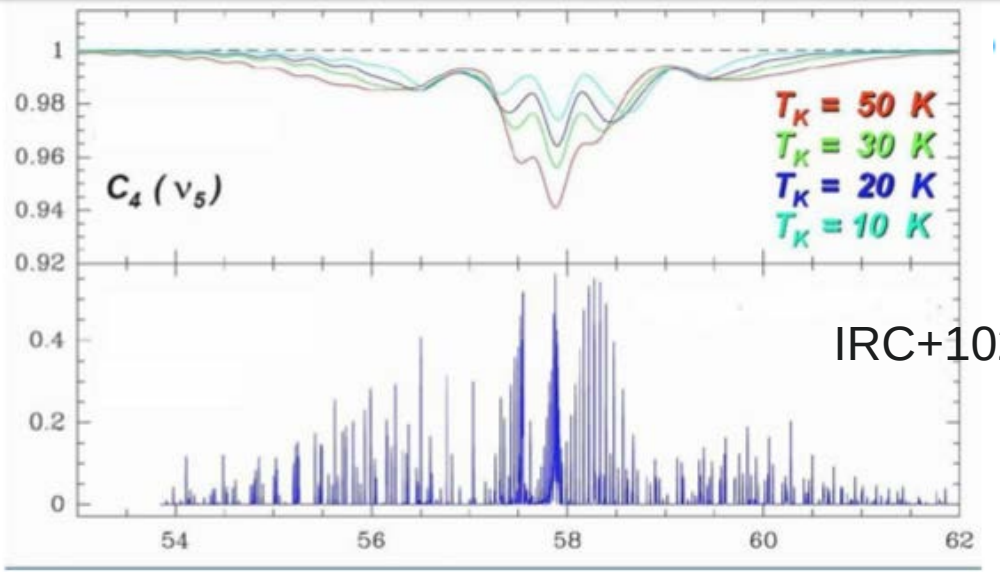

l-C_4 $X^3\Sigma_g^-$;

SiC_3 / C_4

IRC+10216

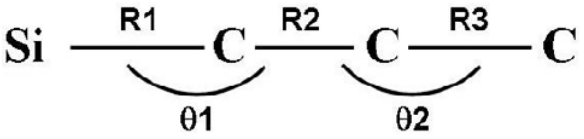

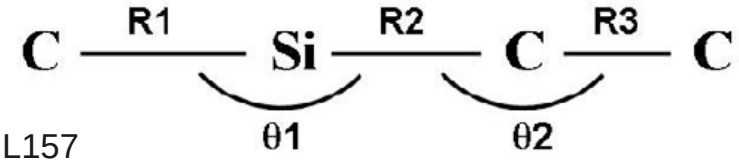

Cernicharo, J., Goicochea, J. R., & Benilan, Y. 2002, ApJ, 580, L157

l-C_4 0.44 eV ($^1\Delta_g$) and 0.61 eV ($^1\Sigma_g^+$)

State	CASSCF/cc-pVTZ[a]	MRCI+Q/cc-pVTZ[b]	MCQDPT[c]	Electron configuration
$X^3\Sigma^-$	0.0	0.0	0.0	$(11\sigma)^2(2\pi)^4(3\pi)^2$
$^1\Delta$	0.30	0.29	0.40	$(11\sigma)^2(2\pi)^4(3\pi)^2$
$^1\Sigma^+$	0.44	0.46	0.46	$(11\sigma)^2(2\pi)^4(3\pi)^2$

N.Inostroza, M.L. Senent, M. Hochlaf, Astronomy &Astrophysics 486, 1047 (2008)

Results

		RCCSD(T) $cc-pVDZ^a$	RCCSD(T) $cc-pVTZ^b$	UCCSD(T) $cc-pVTZ^b$	CASSCF $cc-pVDZ^a$	CASSCF $cc-pVTZ^b$	CASSCF $cc-pVQZ^b$	MCSCF 6-31G(*d*)^c	CCSD(T) cc-pVQZ^d	MP2 6-31G(*d*)^e	CISD DZP^f	$m\omega^g$
R_1	(Si-CCC str)	1.7662	1.7447	1.7427	1.7531	1.7410	1.7197	1.74	1.7249	1.732	1.722	
R_2	(SiC-CC str)	1.3299	1.2959	1.2954	1.2966	1.2841	1.2956	1.29	1.2899	1.297	1.298	
R_3	(SiCC-C str)	1.3120	1.3108	1.3133	1.3111	1.3003	1.2987	1.31	1.3062	1.3111	1.3070	
μ						4.0293	4.4064					
B_e		2636.4	2705.49	2706.86	2691.68	2736.88	2753.16					2747.7085
B_0		2637.8			2690.45							
$D_e \times 10^{-6}$		221.529			218.844							255.23
$\omega_1(\sigma)$	(C-C-C stretching)	2016.2	2040	1971	2070.0	2060	2005 (I = 152)	2055		2003		
$\omega_2(\sigma)$	(Si-C stretching)	1368.8	1391	1318	1357.1	1365	1366 (I = 11)	1342		1332		
$\omega_3(\sigma)$	(C-C-C stretching)	593.8	612	606	611.3	621	639 (I = 4)	613		629		
$\omega_4(\pi)$	(trans-bending)	379.8	384	381	443.1	455	463 (I = 9)	382		380		
$\omega_5(\pi)$	(cis-bending)	147.2	147	147	166.9	175	166 (I = 3)	150		151		

[a] This work. Values derived from our 6D PES; [b] this work. Values obtained using standard approaches implemented in MOLPRO. Refs. (Eckert et al. 1997) (Rauhut et al. 1999); [c] Ref. (Rintelman et al. 2001); [d] Ref. (Sattelmeyer et al. 2002); [e] Ref. (Gomei et al. 1997); [f] Ref. (Alberts et al. 1990); [g] Ref. (McCarthy et al. 2000).

N.Inostroza, M.L. Senent, M. Hochlaf, Astronomy &Astrophysics 486, 1047 (2008)

Results

CHARACTERIZATION of the anion SiC_3H^-

The hydrogen-bearing silicon carbide radicals SiC_nH are isovalent to $C_{n+1}H$ species.

SiC_3H^- isovalent to C_4H^-

C_4H^-

has been one of the first anions detected.

Cernicharo, J. et.al, ApJ. 2002

Neutral C_4H was detected 20 years early.

Results

neutral		μ	*anion*		μ	E_a
CSi	($X^3\Pi$)	0.8831	**l-CSi$^-$**	($X^2\Sigma^+$)	0.6885	**2.42**
c-C_2Si	(X^1A_1)	2.9587	**l-C_2Si$^-$**	($X^2\Pi$)	3.8003	**1.41**
c-C_3Si **l-C_3Si**	(X^1A_1) ($X^3\Sigma^-$)	3.8671 4.4016	**l-C_3Si$^-$**	($X^2\Pi$)	4.1481 --	**2.49** 2.89
l-C_4Si	($X^1\Sigma^+$)	6.2111	**l-C_4Si$^-$**	($X^2\Pi$)	5.9792	**2.31**
l-C_5Si	($X^3\Sigma^-$)	6.4927	**l-C_5Si$^-$**	($X^2\Pi$)	6.0682	**3.30**
l-SiCH	($X^2\Pi$)	0.5771	**l-SiCH$^-$**	($X^1\Sigma^+$)	0.3089	**3.88**
l-SiC_2H	($X^2\Pi$)	1.1201	**l-SiC_2H^-**	($X^3\Sigma^-$)	4.2681	**1.32**
l-SiC_3H	($X^2\Pi$)	1.1074	**l-SiC_3H^-**	($X^1\Sigma^+$)	**2.9949**	**2.70**
l-SiC_4H	($X^2\Pi$)	1.3061	**l-SiC_4H^-**	($X^3\Sigma^-$)	7.3735	**1.69**
l-SiC_5H	($X^2\Pi$)	0.5122	**l-SiC_5H^-**	($X^1\Sigma^+$)	4.8991	**2.98**

Results

neutral		μ	*anion*		μ	E_a
CSi	($X^3\Pi$)	0.8831	**l-CSi$^-$**	($X^2\Sigma^+$)	0.6885	**2.42**
c-C_2Si	(X^1A_1)	2.9587	**l-C_2Si$^-$**	($X^2\Pi$)	3.8003	**1.41**
c-C_3Si **l-C_3Si**	(X^1A_1) ($X^3\Sigma^-$)	3.8671 4.4016	**l-C_3Si$^-$**	($X^2\Pi$)	4.1481 --	**2.49** 2.89
l-C_4Si	($X^1\Sigma^+$)	6.2111	**l-C_4Si$^-$**	($X^2\Pi$)	5.9792	**2.31**
l-C_5Si	($X^3\Sigma^-$)	6.4927	**l-C_5Si$^-$**	($X^2\Pi$)	6.0682	**3.30**
l-SiCH	($X^2\Pi$)	0.5771	**l-SiCH$^-$**	($X^1\Sigma^+$)	0.3089	**3.88**
l-SiC_2H	($X^2\Pi$)	1.1201	**l-SiC_2H$^-$**	($X^3\Sigma^-$)	4.2681	**1.32**
l-SiC_3H	($X^2\Pi$)	1.1074	**l-SiC_3H$^-$**	($X^1\Sigma^+$)	**2.9949**	**2.70**
l-SiC_4H	($X^2\Pi$)	1.3061	**l-SiC_4H$^-$**	($X^3\Sigma^-$)	7.3735	**1.69**
l-SiC_5H	($X^2\Pi$)	0.5122	**l-SiC_5H$^-$**	($X^1\Sigma^+$)	4.8991	**2.98**

Results

neutral		μ	*anion*		μ	E_a
CSi	($X^3\Pi$)	0.8831	**l-CSi$^-$**	($X^2\Sigma^+$)	0.6885	**2.42**
c-C_2Si	(X^1A_1)	2.9587	**l-C_2Si$^-$**	($X^2\Pi$)	3.8003	**1.41**
c-C_3Si **l-C_3Si**	(X^1A_1) ($X^3\Sigma^-$)	3.8671 4.4016	**l-C_3Si$^-$**	($X^2\Pi$)	4.1481 --	**2.49** 2.89
l-C_4Si	($X^1\Sigma^+$)	6.2111	**l-C_4Si$^-$**	($X^2\Pi$)	5.9792	**2.31**
l-C_5Si	($X^3\Sigma^-$)	6.4927	**l-C_5Si$^-$**	($X^2\Pi$)	6.0682	**3.30**
l-SiCH	($X^2\Pi$)	0.5771	**l-SiCH$^-$**	($X^1\Sigma^+$)	0.3089	**3.88**
l-SiC_2H	($X^2\Pi$)	1.1201	**l-SiC_2H$^-$**	($X^3\Sigma^-$)	4.2681	**1.32**
l-SiC_3H	($X^2\Pi$)	1.1074	**l-SiC_3H$^-$**	($X^1\Sigma^+$)	**2.9949**	**2.70**
l-SiC_4H	($X^2\Pi$)	1.3061	**l-SiC_4H$^-$**	($X^3\Sigma^-$)	7.3735	**1.69**
l-SiC_5H	($X^2\Pi$)	0.5122	**l-SiC_5H$^-$**	($X^1\Sigma^+$)	4.8991	**2.98**

Results

neutral		μ	*anion*		μ	E_a
CSi	($X^3\Pi$)	0.8831	**l-CSi$^-$**	($X^2\Sigma^+$)	0.6885	**2.42**
c-C_2Si	(X^1A_1)	2.9587	**l-C_2Si$^-$**	($X^2\Pi$)	3.8003	**1.41**
c-C_3Si **l-C_3Si**	(X^1A_1) ($X^3\Sigma^-$)	3.8671 4.4016	**l-C_3Si$^-$**	($X^2\Pi$)	4.1481 --	**2.49** 2.89
l-C_4Si	($X^1\Sigma^+$)	6.2111	**l-C_4Si$^-$**	($X^2\Pi$)	5.9792	**2.31**
l-C_5Si	($X^3\Sigma^-$)	6.4927	**l-C_5Si$^-$**	($X^2\Pi$)	6.0682	**3.30**
l-SiCH	($X^2\Pi$)	0.5771	**l-SiCH$^-$**	($X^1\Sigma^+$)	0.3089	**3.88**
l-SiC_2H	($X^2\Pi$)	1.1201	**l-SiC_2H$^-$**	($X^3\Sigma^-$)	4.2681	**1.32**
l-SiC_3H	($X^2\Pi$)	1.1074	**l-SiC_3H$^-$**	($X^1\Sigma^+$)	**2.9949**	**2.70**
l-SiC_4H	($X^2\Pi$)	1.3061	**l-SiC_4H$^-$**	($X^3\Sigma^-$)	7.3735	**1.69**
l-SiC_5H	($X^2\Pi$)	0.5122	**l-SiC_5H$^-$**	($X^1\Sigma^+$)	4.8991	**2.98**

Ea → RCCSD(T)-F12A/aug-cc-pVTZ

neutral		μ	*anion*		μ	E_a
CSi	($X^3\Pi$)	0.8831	l-CSi$^-$	($X^2\Sigma^+$)	11.5921	2.42
c-C_2Si	(X^1A_1)	2.9587	l-C_2Si$^-$	($X^2\Pi$)	5.6931	1.41
c-C_3Si l-C_3Si	(X^1A_1) ($X^3\Sigma^-$)	3.8671 4.4016	l-C_3Si$^-$	($X^2\Pi$)	2.4308	2.49 2.89
l-C_4Si	($X^1\Sigma^+$)	6.2111	l-C_4Si$^-$	($X^2\Pi$)	2.2349	2.31
l-C_5Si	($X^3\Sigma^-$)	6.4927	l-C_5Si$^-$	($X^2\Pi$)	5.2765	3.30
l-SiCH	($X^2\Pi$)	0.5771	l-SiCH$^-$	→	0.3089	**3.88**
l-SiC_2H	($X^2\Pi$)	1.1201	l-SiC_2H$^-$	($X^3\Sigma^-$)	1.3651	1.32
l-SiC_3H	($X^2\Pi$)	1.1074	l-SiC_3H$^-$	→	**2.9949**	**2.70**
l-SiC_4H	($X^2\Pi$)	1.3061	l-SiC_4H$^-$	($X^3\Sigma^-$)	10.8913	1.69
l-SiC_5H	($X^2\Pi$)	0.5122	l-SiC_5H$^-$	→	4.8991	**2.98**

C_2H^-

C_4H^-

C_6H^-

neutral		μ	*anion*		μ	E_a
CSi	($X^3\Pi$)	0.8831	l-CSi$^-$	($X^2\Sigma^+$)	11.5921	2.42
c-C_2Si	(X^1A_1)	2.9587	l-C_2Si$^-$	($X^2\Pi$)	5.6931	1.41
c-C_3Si l-C_3Si	(X^1A_1) ($X^3\Sigma^-$)	3.8671 4.4016	l-C_3Si$^-$	($X^2\Pi$)	2.4308	2.49 2.89
l-C_4Si	($X^1\Sigma^+$)	6.2111	l-C_4Si$^-$	($X^2\Pi$)	2.2349	2.31
l-C_5Si	($X^3\Sigma^-$)	6.4927	l-C_5Si$^-$	($X^2\Pi$)	5.2765	3.30
l-SiCH	($X^2\Pi$)	0.5771		($X^1\Sigma^+$)	[illegible]	3.88
l-SiC_2H	($X^2\Pi$)	1.1201	l-SiC_2H$^-$	($X^3\Sigma^-$)	1.3651	1.32
l-SiC_3H	($X^2\Pi$)	1.1074	l-SiC_3H$^-$	($X^1\Sigma^+$)	2.9949	2.70
l-SiC_4H	($X^2\Pi$)	1.3061	l-SiC_4H$^-$	($X^3\Sigma^-$)	10.8913	1.69
l-SiC_5H	($X^2\Pi$)	0.5122	l-SiC_5H$^-$	($X^1\Sigma^+$)	4.8991	2.98

C_4H^-

Results

***l*-SiC$_3$H**

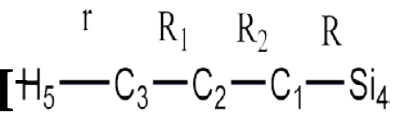

$X^1\Sigma^+$

***c*-SiC$_3$H$^-$**

X^1A'

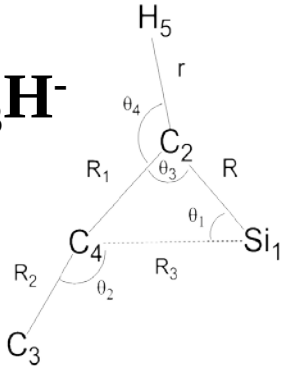

***l1*-SiC$_3$H$^-$**

X^1A'

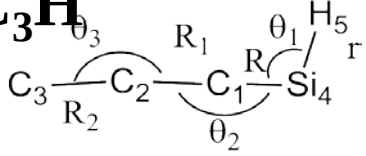

***c1*-SiC$_3$H$^-$**

X^1A'

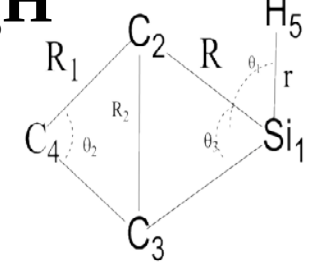

c2-SiC$_3$H$^-$

X^1A'

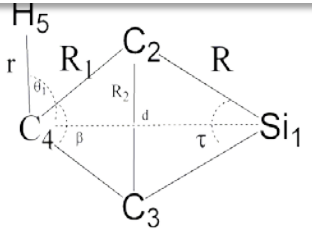

c3-SiC$_3$H$^-$

X^1A'

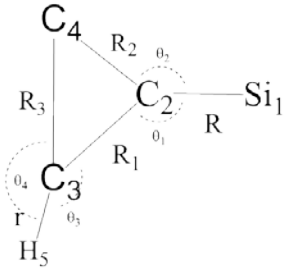

***l2*-SiC$_3$H$^-$**

X^1A'

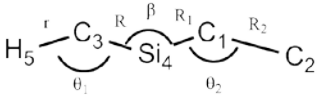

c4-SiC$_3$H$^-$

X^1A

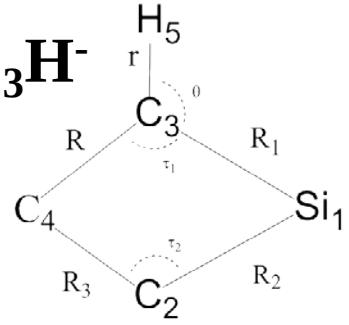

c5-SiC$_3$H$^-$

X^1A'

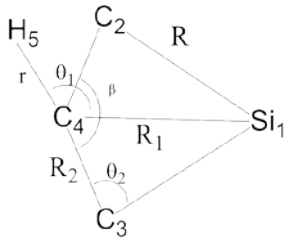

c6-SiC$_3$H$^-$

X^1A'

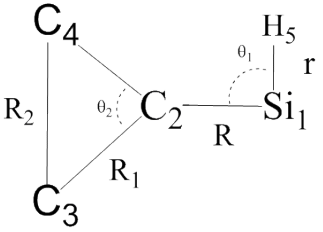

c7-SiC$_3$H$^-$

X^1A'

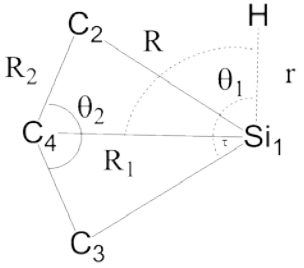

***l3*-SiC$_3$H$^-$**

X^1A'

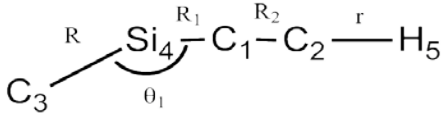

Results

$$B_0 = B_e^{CBS} + \Delta B_e^{core} + \Delta B_{vib}$$

$$\Delta B_e^{core} = B_e(\text{aug-cc-pCVQZ, n=1}) - B_e(\text{aug-cc-pVQZ, n=8})$$

ΔB_e^{core} 17 MHz ΔB_{vib} 2 MHz

B_0 (l-SiC_3H^-)=2620.74 MHz B_0 (l-SiC_3D^-)= 2459.81 MHz

μ= 2.9707 Debyes

CASSCF/aug-cc-pV5Z

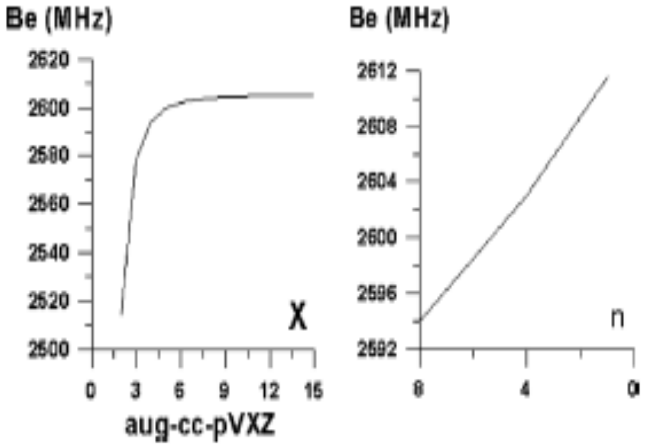

$B_e = B_e^{CBS} + B_e^{1} (X+1)^{-3} + B_e^{2} (X+1)^{-5} + ...$

Basis set	n[a]	l-SiC_3H^- B_e	l-SiC_3D^- B_e
RCCSD(T)-F12A aug-cc-pVTZ	8	2598.33	2438.24
aug-cc-pVTZ	8	2578.13	2419.55
aug-cc-pVQZ	8	2594.03	2434.29
aug-cc-pV5Z	8	2599.57	2439.36
CBS[b]		2605.16	2444.36
aug-cc-pCVQZ	4	2603.00	2442.46
aug-cc-pCVQZ	1	2611.51	2450.45

a) n=number of frozen core orbitals
b) CBS =complete basis set (aug-cc-pV□Z)

Inostroza et al. Journal of chemical physics **133**, 184107 (2010)

Vertical excitation energies of *l*-SiC_3H^-

l-SiC_3H		*l*-SiC_3H^-	
Sym	**Er MRCI**	**Sym**	**Er MRCI**
$X^2\Pi$	**0.0[b]**	**$X^1\Sigma^+$**	**0.0[d]**
$^2\Sigma^+$	2.01	$^1\Pi$	**3.09**
$^2\Delta$	5.66	$^1\Delta$	**3.29**
$^2\Sigma^-$	5.43	$^1\Sigma^-$	**3.22**
$^4\Sigma^+$	3.43	$^3\Sigma^+$	2.48
$^4\Delta$	3.82	$^3\Pi$	3.10
$^4\Sigma^-$	4.19	$^3\Delta$	2.66
$^4\Pi$	2.21	$^3\Sigma^-$	2.85

Ea= 2.70 eV

MRCI/aug-cc-pVTZ

c) Ea=-493.205588 a.u.; d) Ea=-403.597248 a.u.

Vertical excitation energies of *l*-SiC_3H^-

l-SiC_3H		*l*-SiC_3H^-	
Sym	**Er MRCI**	**Sym**	**Er MRCI**
$X^2\Pi$	**0.0[b]**	**$X^1\Sigma^+$**	**0.0[d]**
$^2\Sigma^+$	2.01	$^1\Pi$	**3.09**
$^2\Delta$	5.66	$^1\Delta$	**3.29**
$^2\Sigma^-$	5.43	$^1\Sigma^-$	**3.22**
$^4\Sigma^+$	3.43	$^3\Sigma^+$	2.48
$^4\Delta$	3.82	$^3\Pi$	3.10
$^4\Sigma^-$	4.19	$^3\Delta$	2.66
$^4\Pi$	2.21	$^3\Sigma^-$	2.85

Ea= 2.70 eV

MRCI/aug-cc-pVTZ

c) Ea=-493.205588 a.u.; d) Ea=-403.597248 a.u.

Results

Vertical excitation energies of *l*-SiC_3H^-

l-SiC_3H		*l*-SiC_3H^-	
Sym	**Er(eV) MRCI**	**Sym**	**Er(eV) MRCI**
$X^2\Pi$	**0.0[b]**	**$X^1\Sigma^+$**	**0.0[d]**
$^2\Sigma^+$	2.01	$^1\Pi$	**3.09**
$^2\Delta$	5.66	$^1\Delta$	**3.29**
$^2\Sigma^-$	5.43	$^1\Sigma^-$	**3.22**
$^4\Sigma^+$	3.43	$^3\Sigma^+$	2.48
$^4\Delta$	3.82	$^3\Pi$	3.10
$^4\Sigma^-$	4.19	$^3\Delta$	2.66
$^4\Pi$	2.21	$^3\Sigma^-$	2.85

Ea= 2.70 eV

MRCI/aug-cc-pVTZ

c) Ea=-493.205588 a.u.; d) Ea=-403.597248 a.u.

Reaction Channels and spectroscopic constant of astrophysical relevant silicon-bearing molecules SiC_3H^+ and SiC_3H

Relative stability

SiC_3H		E_r B3LYP	E_r CCSD(T)
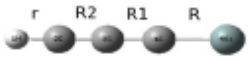	*l1*-SiC_3H $C_{\infty v}$ $X^2\Pi$	0.0	0.0
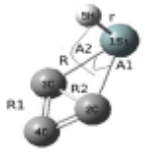	*rb1*- SiC_3H C_1 X^2A'	2.50	2.11
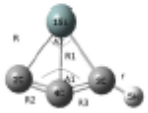	*rb2*-SiC_3H C_s X^2A''	0.62	0.23
	*rb3*-SiC_3H C_{2v} X^2B_1	0.69	0.31

[a] E(B3LYP/cc-pvTZ)= -404.303366 au; [b] E(CCSD(T)/cc-pvTZ)=-403.566239 a

$SiC_3H,^+$		E_r B3LYP	E_r CCSD(T)
	*l1*-SiC_3H^+ $C_{\infty v}$ $X^1\Sigma^+$	0.55	0.93
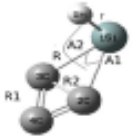	*rb1*-SiC_3H^+ C_s X^1A'	3.58	3.17
	*rb2*-SiC_3H^+ C_s X^1A'	0.82	0.86
	*rb3*-SiC_3H^+ C_{2v} X^1A_1	0.00	0.00

Monthly Notices of the Royal Astronomical Society MNRAS 443, 3127–3133 (2014)

Reaction Channels and spectroscopic constant of astrophysical relevant silicon-bearing molecules SiC_3H^+ and SiC_3H

$X\ ^3\Sigma^-$ l1-SiC_3–1t lies 7.2 kcal mol^{-1}
(0.31 eV)

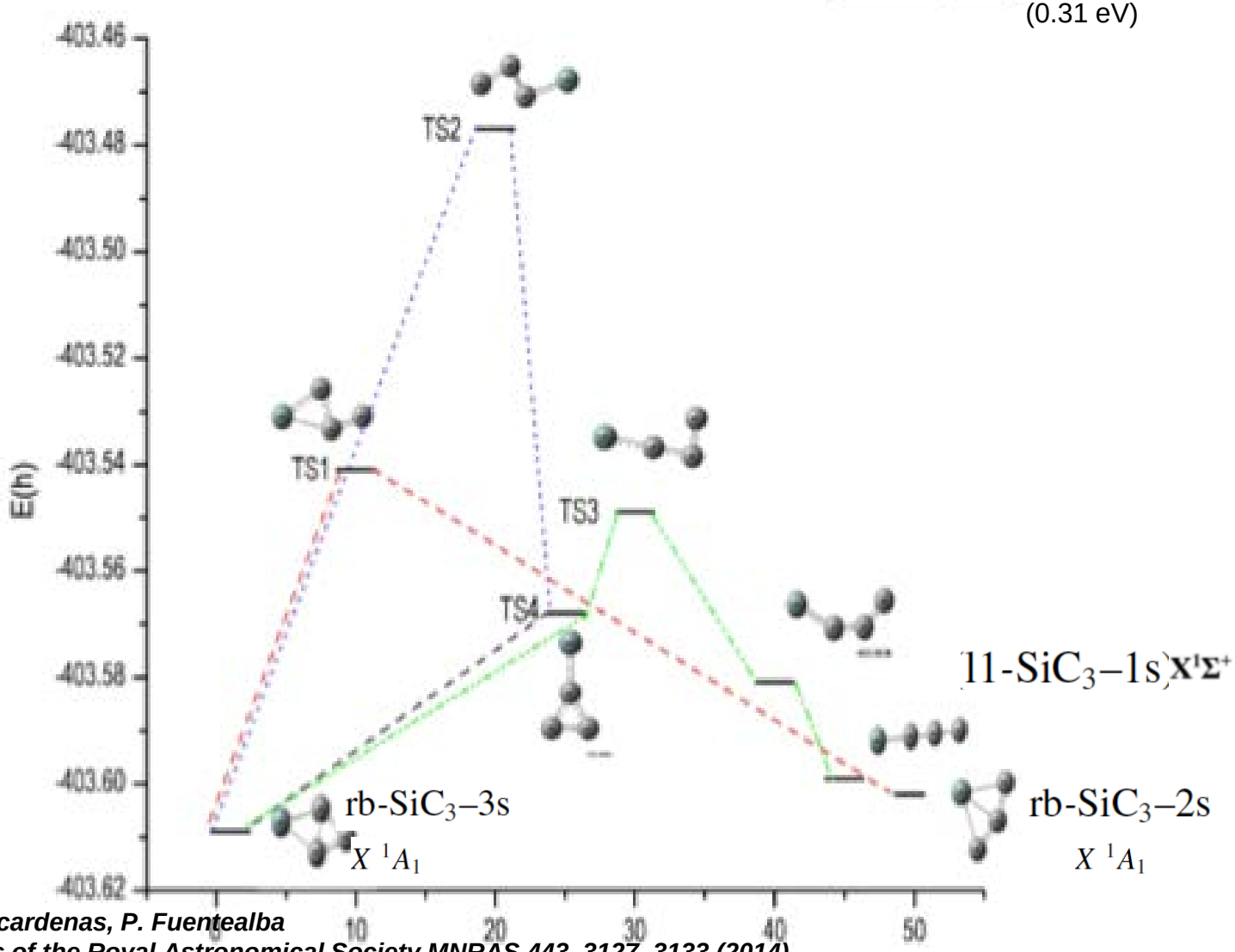

N. INostroza, C.cardenas, P. Fuentealba
Monthly Notices of the Royal Astronomical Society MNRAS 443, 3127–3133 (2014)

Reaction Channels and spectroscopic constant of astrophysical relevant silicon-bearing molecules SiC_3H^+ and SiC_3

Type Reaction		[ΔE(kcal mol^{-1})	ΔE(eV)[a]	[ΔE(kcal mol^{-1})[b]	ΔE (eV)][b]
Charge-exchange (10–300K)	$H^+ + l1\text{-}SiC_3H \rightarrow l1\text{-}SiC_3H^+ + H$	201.5	8.74	203.8	8.84
	$H^+ + rb3\text{-}SiC_3H \rightarrow rb3\text{-}SiC_3H^+ + H$	170.9	7.41	175.4	7.61
	$H^+ + rb2\text{-}SiC_3H \rightarrow rb2\text{-}SiC_3H^+ + H$	192.5	8.35	195.2	8.46
Ion–neutral (10–41 000K)	$H_3^+ + rb\text{-}SiC_3\text{–}3s \rightarrow rb3\text{-}SiC_3H^+ + H_2$	– 126.7	– 5.50	– 129.2	– 5.60
	$H_3^+ + rb\text{-}SiC_3\text{–}3s \rightarrow rb2\text{-}SiC_3H^+ + H_2$	– 106.9	– 4.63	– 109.6	– 4.75
	$H_3^+ + rb\text{-}SiC_3\text{–}3s \rightarrow rb1\text{-}SiC_3H^+ + H_2$	– 53.7	– 2.33	– 46.9	– 2.03
	$H_3^+ + rb\text{-}SiC_3\text{–}2s \rightarrow rb3\text{-}SiC_3H^+ + H_2$	– 132.2	– 5.73	– 135.9	– 5.89
	$H_3^+ + rb\text{-}SiC_3\text{–}2s \rightarrow rb2\text{-}SiC_3H^+ + H_2$	– 112.3	– 4.87	– 114.5	– 4.97
	$H_3^+ + rb\text{-}SiC_3\text{–}2s \rightarrow l1\text{-}SiC_3H^+ + H_2$	– 110.8	– 4.80	– 115.0	– 4.99
	$H_3^+ + l1\text{-}SiC_3\text{–}1t \rightarrow rb3\text{-}SiC_3H^+ + H_2$	– 132.6	– 5.75	– 135.4	– 5.87
	$H_3^+ + l1\text{-}SiC_3\text{–}1t \rightarrow rb2\text{-}SiC_3H^+ + H_2$	– 112.7	– 4.89	– 113.9	– 4.94
	$H_3^+ + l1\text{-}SiC_3\text{–}1t \rightarrow l1\text{-}SiC_3H^+ + H_2$	– 111.2	– 4.82	– 114.4	– 4.96
Dissociative recombination (10–300K)	$rb3\text{-}SiC_3H^+ + e^- \rightarrow rb\text{-}SiC_3\text{–}3s + H$	232.9	10.09	235.1	10.19
	$rb2\text{-}SiC_3H^+ + e^- \rightarrow rb\text{-}SiC_3\text{–}2s + H$	218.5	9.47	220.5	9.56
	$rb2\text{-}SiC_3H^+ + e^- \rightarrow rb\text{-}SiC_3\text{–}3s + H$	212.9	9.23	215.6	9.35
	$l1\text{-}SiC_3H^+ + e^- \rightarrow l1\text{-}SiC_3\text{–}1s + H$	290.1	12.6	281.3	12.2

[a]calculated at CCSD(T)/cc-pvTZ and [b]CCSD(T)/6–311g(d,p) level of theory.

Reaction Channels and spectroscopic constant of astrophysical relevant silicon-bearing molecules SiC_3H^+ and SiC_3H

Charge-exchange (10–300K)	$[\Delta E$(kcal mol^{-1})	ΔE(eV)^a
$H^+ + l1\text{-}SiC_3H \rightarrow l1\text{-}SiC_3H^+ + H$	201.5	8.74
$H^+ + rb3\text{-}SiC_3H \rightarrow rb3\text{-}SiC_3H^+ + H$	170.9	7.41
$H^+ + rb2\text{-}SiC_3H \rightarrow rb2\text{-}SiC_3H^+ + H$	192.5	8.35
Ion–neutral (10–41 000K)		
$H_3^+ + rb\text{-}SiC_3\text{–}3s \rightarrow rb3\text{-}SiC_3H^+ + H_2$	– 126.7	– 5.50

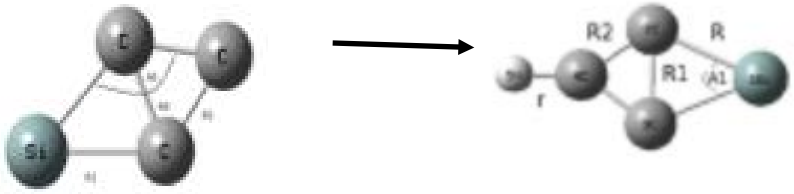

$H_3^+ + rb\text{-}SiC_3\text{–}2s \rightarrow rb3\text{-}SiC_3H^+ + H_2$	– 132.2	– 5.73

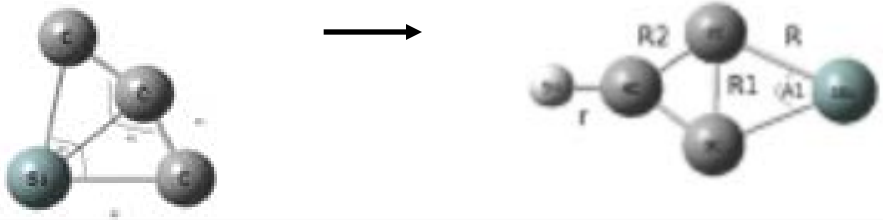

Large amplitude vibrations of Urea in gas phase

N. Inostroza, M.L. Senent *

Departamento de Química y Física Teóricas, Instituto de Estructura de la Materia, IEM-CSIC, Serrano 121, Madrid 28006, Spain

Although Urea rarely appears listed as an interstellar species it constitutes an important prebiotic molecule whose astrophysical detection is always expected. A recent and extensive search towards the high mass hot molecular core Sgr B2 (N–LMH) has been performed with the CARMA and IRAM 30 m radio-telescopes observing several line frequencies coincident with Urea transitions [1]. It has been tentatively detected in infrared spectra of interstellar ices [2].

Chemical Physics Letters 524 (2012) 25–31

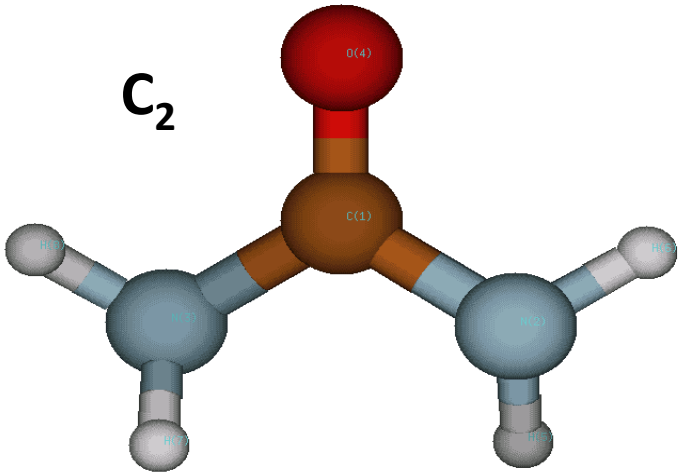

Potential Energy Surface PES

$$V = \frac{1}{2}\sum_i f_{ij} Q_i Q_j + \frac{1}{6}\sum_i \sum_j \sum_k f_{ijk} Q_i Q_j Q_k + \frac{1}{24}\sum_i \sum_j \sum_k \sum_l f_{ijkl} Q_i Q_j Q_k Q_l + \ldots$$

RCCSD(T)-F12/ cc-pVTZ-F12

UREA

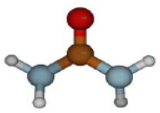

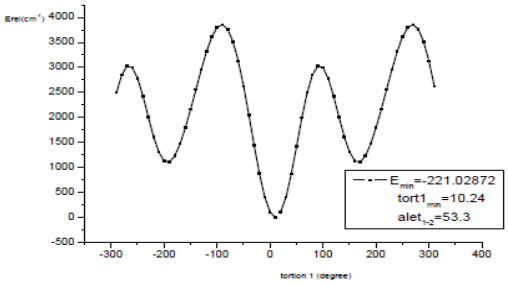

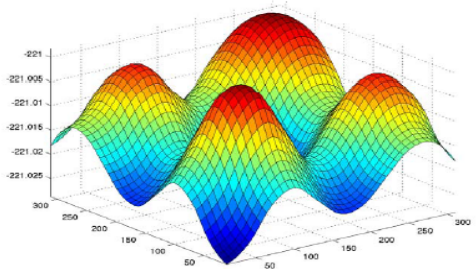

GRID

1409 geometries :

Bond distances $R^{ref}+0.03$ Å ≥ R ≥ $R^{ref}-0.03$Å

Torsional angles $\theta^{ref} + 5.0^o \geq \theta \geq \theta^{ref} - 5.0^o$

Planar bending angles $= \tau + 5.0^o$

FIT

$R^2=1.0$, $\sigma=0.4$ cm^{-1}

FIT-ESPEC (Senent 2007)

Urea

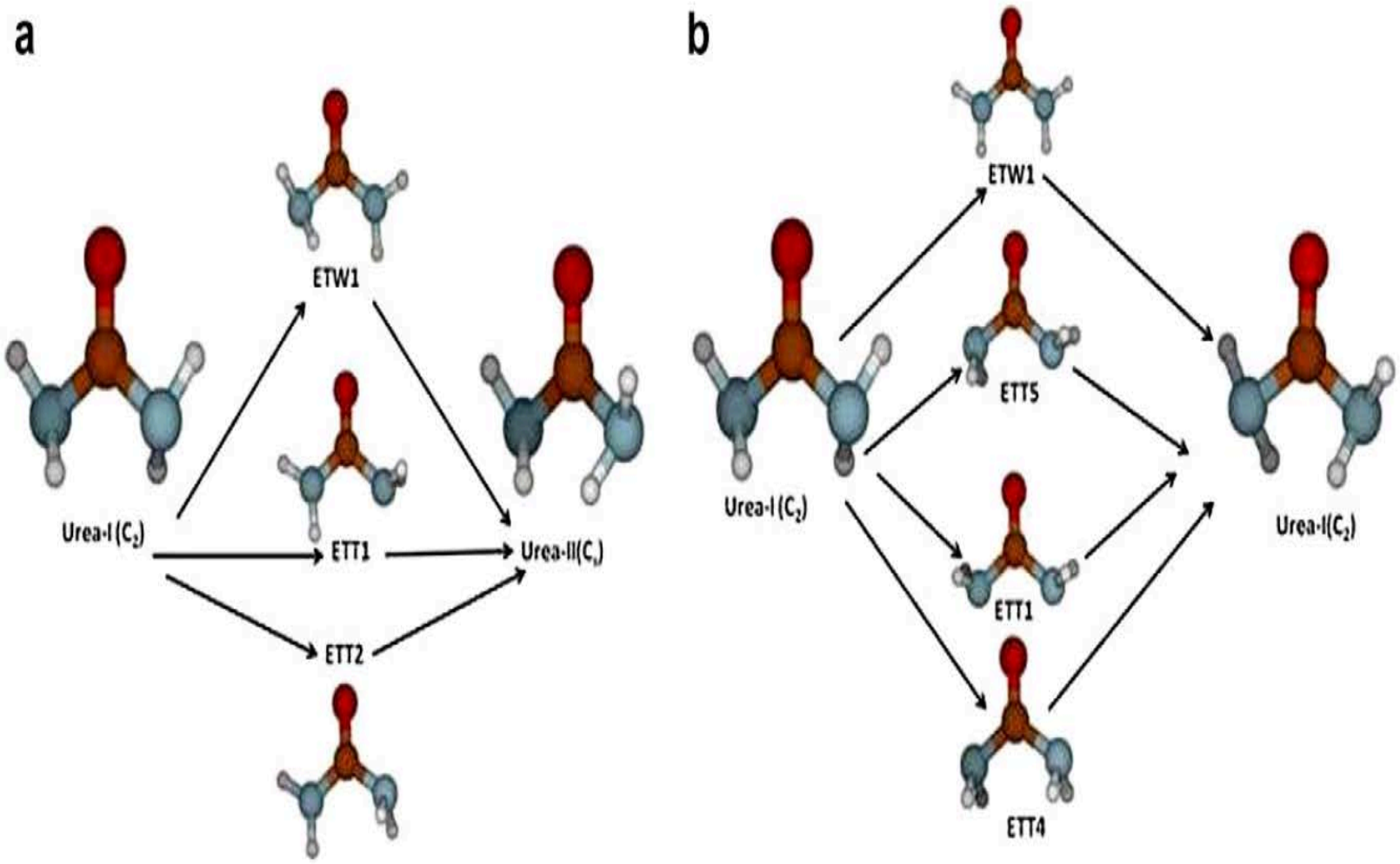

Figure 2. Conversion channels and transition states for the processes (a) Urea-I → Urea-II; (b) Urea-I → Urea-I.

2794 cm^{-1} (torsional barrier) and 395 cm^{-1} (inversion barrier)

Urea I

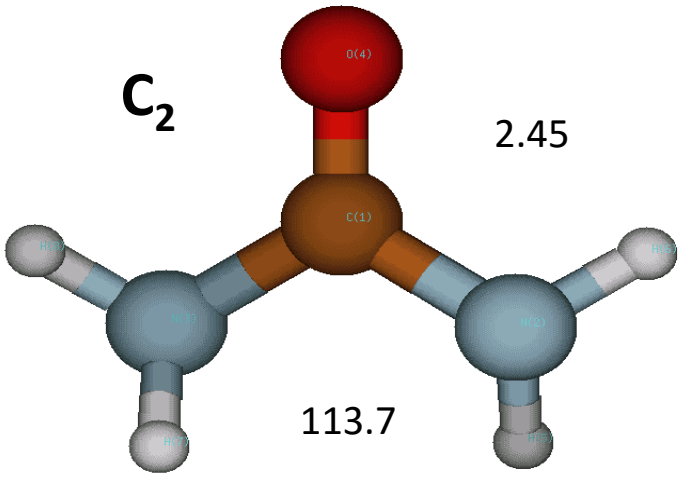

Urea II

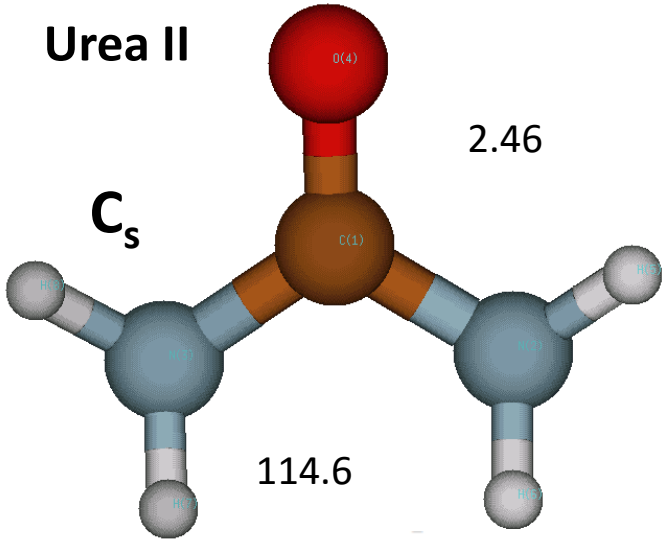

TABLE 1: Total electronic energies (*Ea*, in a.u.), relative energies (E_R, in cm^{-1}), structural parameters (distances in Å; angles in degrees), rotational constants (in MHz) and dipole moments (in Debyes) corresponding to the two conformers of UREA.

	Urea-I (C_2)		Urea-II (C_s)	
aug-cc-pVTZ	**MP2**	**CCSD**	**MP2**	**CCSD-SYM**
E_a	-224.9106098	-224.9217913	-224.9091131	***-224.9191171***
E_R	0.0	0.0	328.48	***510.61***
C-O	1.2191	1.2118	1.2206	***1.2139***
C-N	1.3838	1.3835	1.3789	***1.3777***
N-C-O	123.16	123.11	122.61	***122.85***
H5-N-C	117.14	116.8	120.08	***117.36***
H6-N-C	112.86	112.75	114.11	***117.36***
θ_1	5.7861	5.8338	176.185	***176.82***
β_1	38.5597	39.3752	30.3674	***29.4000***
θ_2	5.7930	5.8349	3.8263	***3.1800***
β_2	38.5606	39.3762	30.3949	***29.4000***
A	11136.50	11229.32	11219.06	***11244.3954***
B	10422.07	10419.66	10393.14	***10458.7141***
C	5433.06	5456.16	5421.96	***5446.2361***
μ	4.03	3.95	4.67	***4.64***

$$\hat{H}_{LAM} = -\sum_{i}^{n}\sum_{i}^{n}\left(\frac{\partial}{\partial_{qj}}\right)B_{ij}\left(\frac{\partial}{\partial_{qj}}\right) + V(q_1, q_2, \ldots, q_n) + V^1(q_1, q_2 \ldots, q_n)$$

Urea

	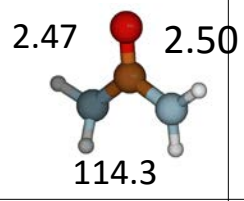	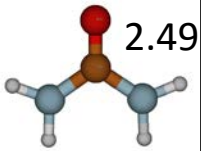	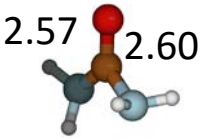	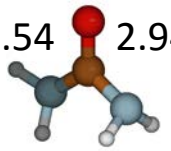	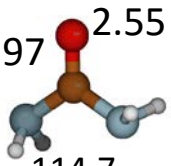	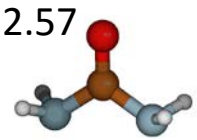	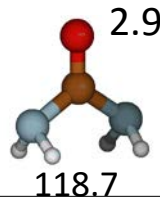
	ETW1	**ETW2**	**ETT1**	**ETT2**	**ETT3**	**ETT4**	**ETT5**
Sym.	C_1	C_{2v}	C_1	C_1	C_s	C_{2v}	C_{2v}
C-O	1.2208	1.2221	1.2158	1.2109	1.2042	1.2100	1.2002
C-N2	1.3860	1.3709	1.4020	1.4067	1.4442	1.4413	1.4475
C-N3	1.3685	1.3708	1.4020	1.4067	1.4442	1.4413	1.4475
N2-C-O	122.75	122.58	124.16	122.44	122.66	123.53	120.67
N3C-O	122.85	122.58	124.16	122.44	122.66	123.53	120.67
H5-N2-C	112.48	123.56	117.67	117.67	106.60	106.57	108.80
H6-N2-C	117.90	116.97	117.67	117.67	106.60	106.57	108.80
H7-N3-C	123.08	123.55	108.40	111.44	106.60	106.57	108.80
H8-N3-C	117.32	116.98	108.40	111.44	106.60	106.57	108.80
θ_1	6.4090	0.0	1.247	3.040	270.0	90.0	270.0
β_1	38.120	0.0	33.862	33.358	62.662	62.601	58.161
θ_2	1.0780	0.0	90.0	270.0	90.00	90.0	270.0
β_2	0.000	0.0	55.654	48.895	62.662	62.601	58.161
μ	**4.5140**	**4.7095**	**2.8386**	**4.9981**	**3.2763**	**0.2148**	**5.2990**
E_a	-224.90921	-224.90834	-224.89205	-224.88606	-224.86408	-224.85917	-224.85917
E_R	**306.4**	**497.7**	**4072.6**	**5388.4**	**10212.2**	**10660.9**	**11290.5**

Urea

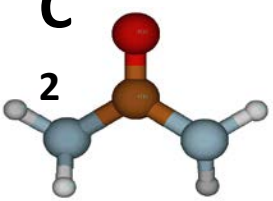

Urea-I (C_2)

Sym	MP2		CCSD(T)	exp	Assign.
	ω	ν	ω	[19]	
A	3723	3560	3685	3559	NH stretch
A	3600	3452	3573	3460	NHstretch
A	1800	1757	1789	1776	CO stretch
A	1635	1592	1639	1604	HNH ben
A	1183	1150	1191	1157	HNH ben
A	959	942	949	1032	CN stretch
A	**575**	**421**	**602**	**582.4**[b]	**NH2 wag**
A	475	472	472		NCN ben
A	**377**	**338**	**377**		**Torsion**
B	3723	3560	3685	3533	NHstretch
B	3595	3450	3570	3434	NHstretch
B	1640	1594	1645	1749	HNH ben
B	1420	1384	1417	1394	CN stretch
B	1057	1011	1064	1157	HNH ben
B	782	726	784	775	CO wag
B	581	556	582	571	NCO ben
B	**545**	**495**	**547**	**550.6**[b]	**NH2 wag**
B	**450**	**380**	**450**	**445.1**[b]	**Torsion**
ZPVE	**14060**	**13420**	**14011**		

[a] Basis set: aug-cc-pVTZ; *ZPVE* and LAM frequencies, in bold.
[b] Experiments in Ar-matriz [15].

Accurate ab initio quartic force fields of cyclic and bent HC2N isomers

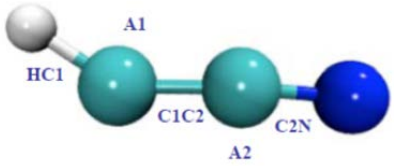

X^3A'' ground state triplet

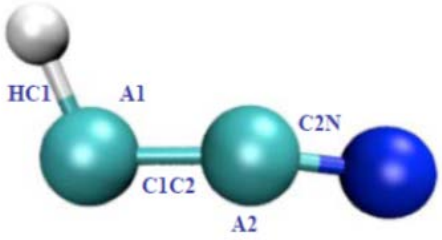

X^1A' bent singlet

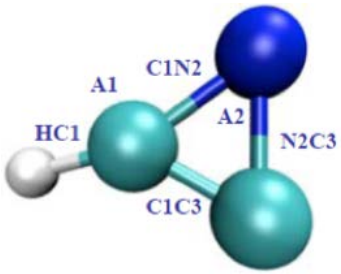

X^1A' cyclic singlet

The grids for each electronic state consisted of 743 distinct geometries and these were used to fit our best QFFs. **CCSD(T)** or **RCCSD(T)** /**cc-pVX Z, X = 3,4,5,**

$$E(l) = E(TQ5) + E(rel - nrel) + E(mtcc - nmtcc),$$

scalar relativistic effects core-correlation correction

The QFFs were used together with second-order **perturbation theory (PT) (SPECTRO)** and **variational methods (MULTIMODE)** to solve the nuclear Schrödinger equation.

Natalia Inostroza , Xinchuan Huang , and Timothy J. Lee. J. Chem. Phys. 135 , 244310 (2011)

Accurate ab initio quartic force fields of cyclic and bent HC2N isomers

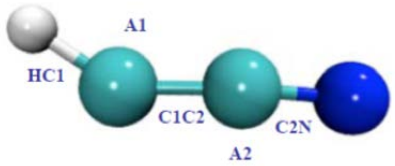

X^3A'' ground state triplet

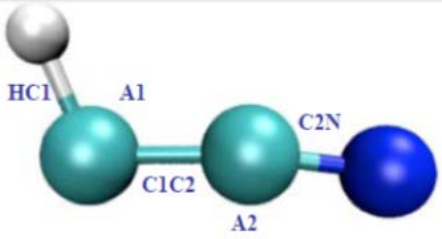

X^1A' bent singlet

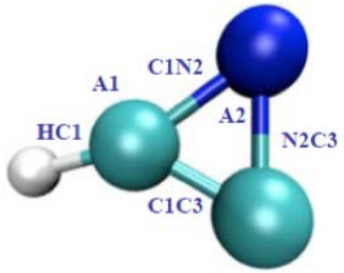

X^1A' cyclic singlet

Isomeric energy differences

HC_2N	ΔE^a	ΔE^b	μ^c
Ground state triplet	0.0	0.0	3.05
Cyclic singlet	5.7	7.8	3.06
Bent singlet	10.6	11.1	1.71

[a]Energies came from the best *ab intio* QFFs, 3-pt(tz,qz,5z)+core+rel.
[b]Includes anharmonic zero-point energies corrections.
[c]Dipole moments computed at CCSD(T)/cc-pVQZ level of theory.

Relative energies (in kcal/mol)

Natalia Inostroza , Xinchuan Huang , and Timothy J. Lee. J. Chem. Phys. 135 , 244310 (2011)

Accurate ab initio quartic force fields of cyclic and bent HC2N isomers

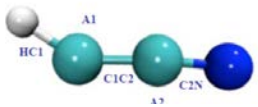

X^3A'' ground state triplet

	PT						VCI		
Ground state triplet	2-pt (tz,qz)	2-pt (qz,5z)	3-pt (tz,qz,5z)	5z +core+rel	3-pt (tz,qz,5z) +core	3-pt (tz,qz,5z) +core+rel	3-pt (tz,qz,5z) +core+rel	Previous work Experiment	Previous work Theory
A_0	2 586 574	2 518 363	2 496 121	2 611 229	2 632 677	2 614 091		4 350 000[b]	10 938.6[e]
B_0	11 016	11 001	10 995	11 037	11 040	11 043		11 027[b]	
C_0	10 951	10 935	10 928	10 972	10 975	10 979		10 986.41[a] 10 986.4[b]	
D_J	0.0042	0.0042	0.0042	0.0042	0.0042	0.0042		0.0041[b]	

A_o	2614091	4350000(b)	
B_o	11043	11027(b)	
C_o	10979	10986.41(a) 1098 6.4(b)	10938.6(c)

Accurate ab initio quartic force fields of cyclic and bent HC2N isomers

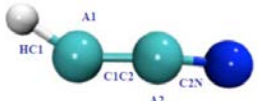

	This Work		Previous Work	
	PT 3-pt (tz,qz,5z) +core+rel	VC 3-pt (tz,qz,5z) +core+rel	Experiment	Theory
υ_1(A')	3243.2	3271.2	3229.0(c)- 3247(d)	3246.66(e)3245.2(f)
υ_2(A')	1722.8	1615.5&	1735(c)-1727, 1735,	1733.71(e)1851.0(f)
υ_3(A')#	1159.3	1177.4	1757(d)	1178.57(e)1113.9(f)
υ_4(A')a1	276.6	305.8	1178(c)	610.4(f)
υ_5(A')	489.0	556.2	458(c)-383(d)-365(a)	336.2(f)
υ_6(A'')	476.8	561.4	369(c)-187(d)-145(a)	362.1(f)

a)From microwave spectra ref. [23]; b) From microwave spectra ref. [17]; c) From argon matrix IR spectra ref. [16] d) From High resolution infrared spectra ref. [25]; e) MR-ACPF/cc-pVQZ; f) From ref. [34] at CASSCF/DZP

Accurate ab initio quartic force fields of cyclic and bent HC2N isomers

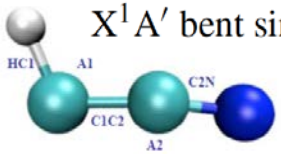

X^1A' bent singlet	PT						VCI
	2-pt (tz,qz)	2-pt (qz,5z)	3-pt (tz,qz,5z)	5z +core+rel	3-pt (tz,qz,5z) +core	3-pt (tz,qz,5z) +core+rel	3-pt (tz,qz,5z) +core+rel
A_0	540 126	539 186	538 717	542 306	543 795	543 130	
B_0	11 069	11 052	11 045	11 093	11 098	11 099	
C_0	10 833	10 816	10 809	10 857	10 861	10 863	
HC1	1.1065	1.1067	1.1069	1.1406	1.1048	1.1049	
C1C2	1.3910	1.3920	1.3924	1.3913	1.3881	1.3881	
C2N	1.1765	1.1777	1.1782	1.1755	1.1758	1.1756	
A1(HC1C2)	109.49	109.41	109.38	108.59	109.70	109.64	
A2(C1C2N)	172.44	172.43	172.43	172.46	172.52	172.49	
$10^9 H_J$	−1.9452	−1.9856	−1.9954	−1.9573	−1.9578	−1.9741	
H_K	0.4942	0.4802	0.4749	0.5040	0.5156	0.5083	
$10^6 H_{JK}$	2.4776	2.5099	2.5173	2.4845	2.4918	2.5012	
H_{KJ}	−0.0020	−0.0021	−0.0021	−0.0021	−0.0021	−0.0021	
$10^{11} h_1$	6.7268	6.5112	6.4392	6.7592	6.8086	6.7709	
$10^{10} h_2$	1.5934	1.5959	1.5957	1.5935	1.5925	1.5988	
$10^{11} h_3$	3.2622	3.2423	3.2350	3.2604	3.2545	3.2630	
D_J	0.0050	0.0050	0.0050	0.0051	0.0050	0.0051	
D_K	228.25	225.56	224.45	231.19	233.91	232.41	
D_{JK}	0.9403	0.9373	0.9360	0.9444	0.9461	0.9459	
$10^3 d_1$	−0.0868	−0.0868	−0.0868	−0.0867	−0.0864	−0.0867	
$10^3 d_2$	−0.0214	−0.0213	−0.0212	−0.0214	−0.0213	−0.0213	
$\upsilon_1(A')$[a]	2928.8	2926.7	2925.8	2932.9	2935.3	2933.8	2934.9
$\upsilon_2(A')$[b]	2043.3	2045.1	2045.3	2048.7	2050.9	2050.7	2050.0
$\upsilon_3(A')$	1040.4	1042.5	1042.8	1044.4	1045.0	1046.9	1046.9
$\upsilon_4(A')$[c]	949.1	956.8	958.3	953.8	957.5	958.4	957.0
$\upsilon_5(A')$	310.4	321.1	323.3	318.3	325.9	325.1	323.9
$\upsilon_6(A'')$	443.2	442.6	442.3	445.4	446.1	445.7	444.2

[a]Fermi resonance type 2 $\upsilon_1 = \upsilon_2 + \upsilon_4$.

Accurate ab initio quartic force fields of cyclic and bent HC2N isomers

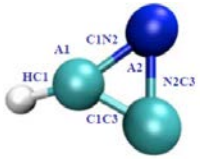

X^1A' cyclic singlet	PT						VCI
	2-pt (tz,qz)	2-pt (qz,5z)	3-pt (tz,qz,5z)	5z +core+rel	3-pt (tz,qz,5z) +core	3-pt (tz,qz,5z) +core+rel	3-pt (tz,qz,5z) +co re+rel
A_0	40 710	40 599	40 557	40 715	40 755	40 744	
B_0	34 414	34 347	34 322	34 489	34 497	34 505	
C_0	18 584	18 541	18 525	18 607	18 618	18 618	
HC1	1.0798	1.0799	1.0800	1.0787	1.0786	1.0786	
C1N2	1.3005	1.3020	1.3026	1.2998	1.2997	1.2996	
N2C3	1.4152	1.4171	1.4179	1.4148	1.4138	1.4141	
C1C3	1.4066	1.4082	1.4087	1.4052	1.4050	1.4047	
A1(HC1N2)	137.87	137.84	137.84	137.93	137.97	137.94	
A2(C1N2C3)	62.22	62.21	62.20	62.18	62.20	62.18	
10^7H_J	−2.8738	−2.9026	−2.9074	−2.8896	−2.9053	−2.9132	
10^6H_K	18.495	18.533	18.596	18.619	18.153	18.336	
10^6H_{JK}	6.5936	6.6283	6.6488	6.6516	6.5510	6.6001	
10^6H_{KJ}	−21.723	−21.796	−21.876	−21.910	−21.399	−21.605	
$10^{10}h_1$	801.93	792.82	793.75	810.24	781.45	789.14	
$10^{10}h_2$	1886.4	1886.4	1885.4	1891.1	1892.1	1895.6	
$10^{10}h_3$	−347.91	−353.36	−357.60	−359.28	−337.83	−345.77	
D_J	0.0471	0.0469	0.0469	0.0470	0.0472	0.0472	
D_K	0.0904	0.0885	0.0876	0.0882	0.0902	0.0893	
D_{JK}	0.0954	0.0961	0.0966	0.0970	0.0949	0.0960	
d_1	−0.0263	−0.0263	−0.0263	−0.0264	−0.0264	−0.0264	
d_2	−0.0090	−0.0090	−0.0090	−0.0090	−0.0090	−0.0090	
$\upsilon_1(A')$[a]	3122.7	3118.6	3117.4	3126.1	3125.8	3124.7	3126.0
$\upsilon_2(A')$[b]	1571.1	1567.0	1565.7	1572.8	1573.9	1572.5	1576.5
$\upsilon_3(A')$	1292.0	1288.6	1287.6	1294.4	1294.1	1293.6	1294.1
$\upsilon_4(A')$	1012.5	1012.0	1011.6	1013.7	1015.9	1015.1	1014.4
$\upsilon_5(A')$	823.9	821.3	820.4	825.1	825.9	824.9	832.4
$\upsilon_6(A'')$	899.6	894.5	893.3	898.8	896.4	896.0	901.3

[a]Fermi resonance type 1 $\upsilon_1 = 2\upsilon_2$.
[b]Fermi resonance type 2 $\upsilon_2 = 2\upsilon_6$.

Natalia Inostroza, Xinchuan Huang , and Timothy J. Lee. J. Chem. Phys. 135 , 244310 (2011)

ROVIBRATIONAL SPECTROSCOPIC FOR ISOTOPOLOGUES OF CYCLIC AND BENT SINGLET HC2N ISOMERS

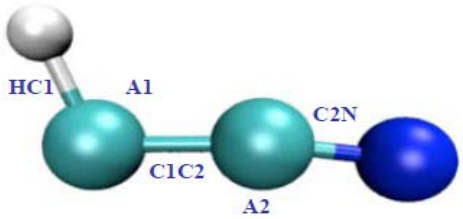

H13CCN	HC13CN	DCCN	HCC15N

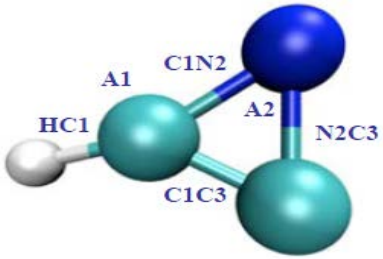

DCNC	H13CNC	HC15NC	HCN13C

Natalia Inostroza , R. Fortenberry , X. Huang , and Timothy J. Lee, The Astrophysical Journal, 778:160 (7pp), 2013 December

ROVIBRATIONAL SPECTROSCOPIC FOR ISOTOPOLOGUES OF CYCLIC AND BENT SINGLET HC2N ISOMERS

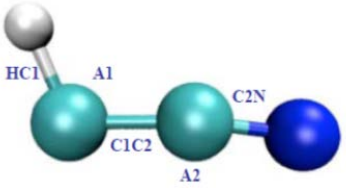

X^1A' bent singlet

CcCR Rotational Constants (MHz), and Fundamental Vibrational Frequencies (cm^{-1}) for the Bent, Singlet HC_2N Isomer Isotopologues

	DCCN		$H^{13}CCN$		$HC^{13}CN$		$HCC^{15}N$	
A_0	307257		537301		542421		543095	
B_0	10366		10695		11099		10755	
C_0	10010		10473		10862		10533	
	VPT2[a]	VCI	VPT2[b]	VCI	VPT2[c]	VCI	VPT2[b]	VCI
ν_1 (a')	2187.4	2187.2	2925.5	2925.4	2936.1	2932.9	2933.2	2933.5
ν_2 (a')	2042.3	2041.0	2043.3	2042.4	2016.0[d]	2015.5[d]	2031.5	2029.6
					1948.0[d]	1950.5[d]		
ν_3 (a')	1001.6	1001.3	1035.9	1034.6	1043.1	1042.8	1039.6	1039.3
ν_4 (a')	797.1	797.7	939.6	938.7	952.8	950.4	956.8	954.1
ν_5 (a')	311.5	309.7	323.8	320.6	316.8	313.9	323.3	320.2
ν_6 (a'')	401.7	401.1	444.4	442.4	436.1	434.3	443.0	441.1

Notes.

[a] The $\nu_2 = 2\nu_3$, $\nu_4 = 2\nu_6$, and $\nu_6 = 2\nu_5$ Fermi resonances are included.

[b] $\nu_1 = \nu_2 + \nu_4$, $\nu_2 = 2\nu_3 = 2\nu_4 = \nu_4 + \nu_3$, $\nu_3 = 2\nu_6$, and $\nu_4 = 2\nu_6$ Fermi resonance polyads.

[c] Require the $\nu_1 = \nu_2 + \nu_4$, $\nu_4 = 2\nu_6$, and $\nu_2 = 2\nu_3 = 2\nu_4 = \nu_4 + \nu_3$ Fermi resonance polyads.

[d] These states are coupled at 50%–50% from the $\nu_2 = \nu_4 + \nu_3$ and $\nu_2 = 2\nu_3$ bases.

ROVIBRATIONAL SPECTROSCOPIC FOR ISOTOPOLOGUES OF CYCLIC AND BENT SINGLET HC2N ISOMERS

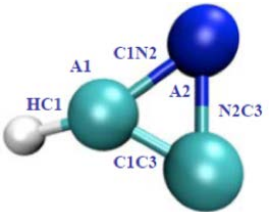

X^1A' cyclic singlet

CcCR Rotational Constants (MHz) and Fundamental Vibrational Frequencies (cm^{-1}) for the Cyclic, Singlet HC_2N Isomer Isotopologues

	DCCN		$H^{13}CCN$		$HC^{13}CN$		$HCC^{15}N$	
A_0	42505		43549		41784		43783	
B_0	27137		31172		31934		30843	
C_0	16508		18106		18038		18034	
	VPT2[a]	VCI	VPT2[b]	VCI	VPT2[b]	VCI	VPT2[b]	VCI
ν_1 (a')	2364.2	2364.8	3125.4	3123.3	3146.6	3139.7	3137.9	3135.7
ν_2 (a')	1530.7	1535.8	1548.0	1551.3	1565.0	1569.4	1552.8	1556.3
ν_3 (a')	1270.3	1271.0	1272.9	1273.5	1274.4	1274.9	1288.6	1289.2
ν_4 (a')	961.9	965.6	1011.3	1010.3	1003.1	1002.2	1004.6	1003.6
ν_5 (a')	665.7	669.6	821.9	829.5	817.5	825.0	820.3	827.8
ν_6 (a'')	712.3	715.5	888.2	893.4	895.2	900.6	895.8	901.1

Notes.

[a] Fermi resonance $\nu_1 = 2\nu_3$, $\nu_2 = 2\nu_6$, and $\nu_3 = 2\nu_6$.

[b] Fermi resonance $\nu_1 = 2\nu_2$ and $\nu_2 = 2\nu_5$.

Natalia Inostroza , R. Fortenberry , X. Huang , and Timothy J. Lee, The Astrophysical Journal, 778:160 (7pp), 2013 December

Low-Lying Electronic States of the Quasi-Linear ($^3A''$) and Cyclic ($^1A'$) Isomers of Cyanomethylene HCCN

Natalia Inostroza-Pino[1], Partha P. Bera[2,3], Xinchuan Huang[2,4], and Timothy J. Lee[2]*

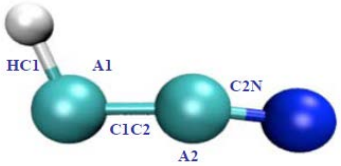

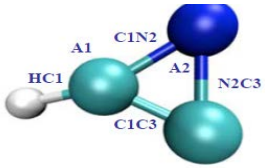

Electronic excitations energies and oscillator strengths of the quasi-linear ground triplet state $^3A'$ HCCN and singlet cyclic $^1A'$ *c*-HCCN isomers were computed using EOM-CCSDT
B3LYP and ωB97-X , CIS CIS(D) //cc-pVXZ, aug-cc-pVXZ and d-aug-cc-pVXZ (X=T or Q) basis sets. Electronic excitation energies : both isomers show intense ultraviolet-visible (UV-Vis) spectra for electronic transitions with large oscillator strengths at the B3LYP, ωB97-X, and equations-of-motion coupled cluster levels.

The triplet ground state is a floppy molecule, letting a conjugation between π-electron of the CN bond to the electrons of the HC-part. Due to this, it is expected that a mixture of $^3A''$ and $^3\Sigma$- electronic states would produce lines in the visible region of the electromagnetic spectrum.

Natalia Inostroza ,P. Bera, Xinchuan Huang , and Timothy J. Lee submitted June 2016

In dust we trust ??

$$CH_3OH + OH \rightarrow CH_3O + H_2O,$$

$$CH_3OH + OH \rightarrow CH_2OH + H_2O.$$

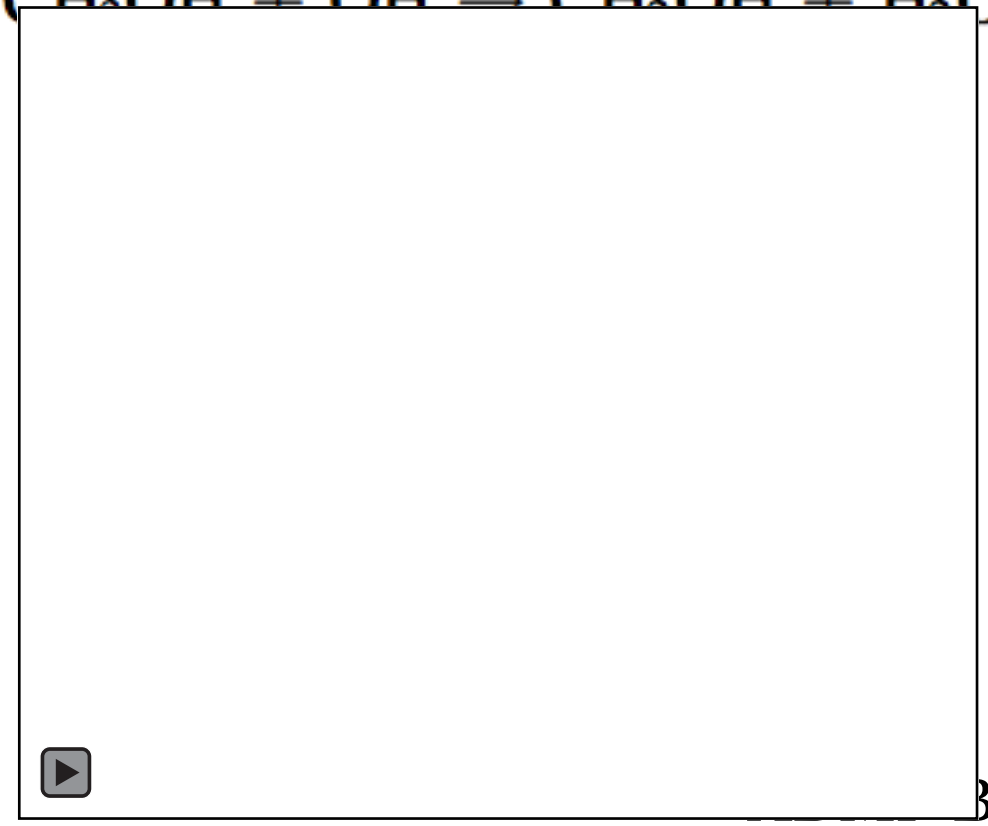

B3LYP-6-31G

UNIVERSIDAD AUTONOMA DE CHILE

BOMD
30K

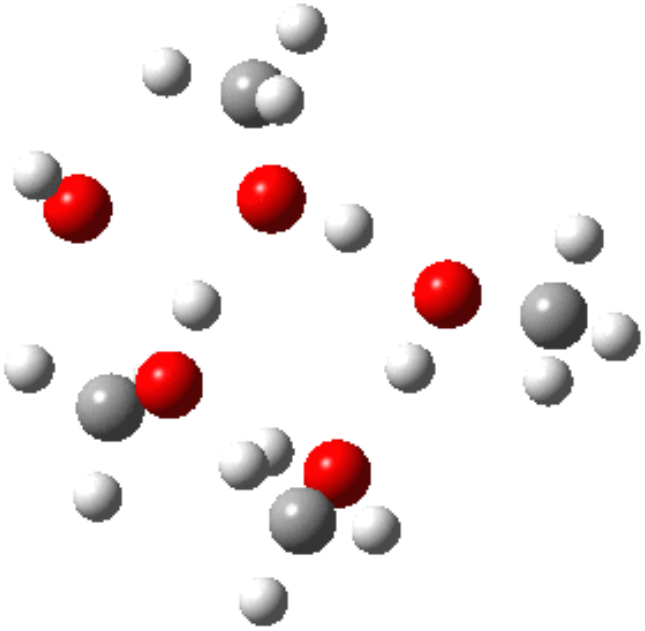

The gas-phase reaction between OH and CH3OH is an important contributor to the formation of interstellar CH3O. The role of grain-surface processes in the formation of CH3O, although it cannot be fully neglected, remains controversial


Astrochemistry school, May 2016

CALAN OBSERVATORY

Group of Molecular Astrophysics at ICMM-CSIC,

IAUS 332: Astrochemistry VII

Through the Cosmos from Galaxies to Planets

March 20 to 24, 2017

Puerto Varas CHILE

http://newt.phys.unsw.edu.au/~marciac/IAUS332/

UNIVERSIDAD AUTONOMA DE CHILE

International Symposium and Workshop on Astrochemistry-Campinas July 3-8

Thanks for you attention